

Z-Selective Multi-Spectral 3D Imaging: A MAVRIC-SEMAC Hybrid

K. M. Koch¹, K. F. King¹, B. A. Hargreaves², and G. C. McKinnon¹

¹Applied Science Laboratory, GE Healthcare, Waukesha, WI, United States, ²Department of Radiology, Stanford University, Palo Alto, CA, United States

Introduction: Two recently developed sequences, MAVRIC and SEMAC, have been shown to significantly reduce susceptibility artifacts near metallic implants [1,2]. The two techniques are conceptually very similar, despite differences in implementation. Here, we show that advantageous elements of both techniques can be combined to further improve upon their individual capabilities.

Theory: The Multiple-Acquisitions with Variable Resonance Image Combination (MAVRIC) technique is a 3D method that builds composite images from multiple acquisitions with spatially non-selective RF excitations of varying frequency offsets [1]. The Slice Encoding for Metal Artifact Correction (SEMAC) technique excites 2D slices, performs a 3D acquisition, and uses view-angle-tilting [3] to reduce in-plane distortions [2]. Unlike MAVRIC, the use of z-selection during RF application provides an element of volume selectivity to the SEMAC technique. This fact is illustrated in Figure 1, where the MAVRIC spectral bins are spatially independent, whereas the SEMAC bins are tilted along the frequency/position axis.

As also demonstrated in Figure 1, MAVRIC and SEMAC apply differing RF pulses and spectral arrangements. Briefly, this choice is between (a) overlapping spectral profiles that, when summed, provide a unit response, or (b) closely matched flat-top excitation profiles arranged adjacently to one another. MAVRIC utilizes (a) while SEMAC uses (b).

Spatial B₁ modulations found around metal implants and imperfect slice profiles can result in signal gaps or intensity spikes near boxcar profiles. Overlapping profiles reduce such artifacts, but require 2 TR periods to reduce cross-excitation. However, SNR is improved, and longer echo-train lengths can compensate for scan time.

A procedure is now described to construct an acquisition sequence that possesses the spectral overlap of MAVRIC and the z-selectivity of SEMAC.

Consider a MAVRIC acquisition with N spectral bins (or acquisitions) and a spectral bin separation of Q kHz. We desire to restrict the excited z FOV to ΔZ cm. This can be accomplished by applying the MAVRIC excitations under a z-gradient of amplitude $G_z = 2\pi N * Q / (\gamma \Delta Z)$. As in SEMAC, the z-gradient must also be turned on during the readout process in order to keep off-resonance effects limited to the RF bandwidth [4].

Using this strategy, like SEMAC, the resolution in the z-dimension is not determined by the selective z-gradient amplitude, but by the number of z phase-encodes. Since multiple z-encodes are performed in each excitation, the view-angle is also much lower than that used in an equivalent 2D experiment. In the context of Figure 1, this hybrid method has an increased position vs frequency slope compared to the SEMAC diagram, but uses the overlapping RF spectral arrangement indicated in the MAVRIC diagram.

Results : Figure 2 a-f presents the variation of excitation volumes and composite images when applying the z-gradient in the presence of a sample implant-induced B₀ distribution. Here Gaussian RF pulses of FWHM = 2.25 kHz are applied to excite spectral bins separated by Q=1 kHz near a total hip replacement at 1.5T. The volumes (projected in the ky-kz encoded plane) excited without the use of a z-gradient are displayed (a-c) for the -4 kHz, 0kHz, +4kHz spectral bins. The non-selective composite image is shown in (d). It is clear that the 0kHz bin (b) in this case is susceptible to phase-encode aliasing (arrows). When the appropriately scaled z-gradient is applied (e-h), the excited volumes are all selective in z, eliminating the threat of phase-encode aliasing in this dimension. The reduction of aliasing is clearly visible in the composite images (d,h). Figure 2 (i-k) display the in-plane images for (i) 2D-FSE, (j) non-selective multispectral 3D, (k) z-selective multispectral 3D (all acquired at +/- 125 kHz readout bandwidth). It is clear that both (j) and (k) correct the susceptibility artifacts found in (i). There is not any significant change of the artifact reduction found in (j) when the z-selective process (k) is utilized. Close examination of the plastic phantom gridlines in (k) shows a shear relative to those in (i) and (j). This is an anticipated effect of the view-angle tilting process and is why minimization of the view-angle is an important consideration. Figure 3 further displays *in-vivo* results near a stainless steel ankle screw at 3T. Notice that the view-angle tilting shearing effect seen in Figure 2 is not easily identifiable in the *in vivo* images as these effects depend on orientation of structures. The distortions identified in the 2D-FSE images (a,d) are clearly repaired in the both multispectral 3D acquisitions (b,c,e,f). In addition, the aliasing found in the conventional MAVRIC images (b,e) are completely removed in the z-selective hybrid images (c,e).

Conclusions: We have demonstrated that the z-selectivity of SEMAC can be merged with the spectrally overlapping 3D encoding strategies of MAVRIC. Both techniques mitigate susceptibility artifacts through use of z phase-encoding and reducing off-resonance contributions to individual Fourier reconstructions. This similarity enables the sharing of features between the two methods.

[1] Koch et al, MRM,61,2009, 381-390, [2] Lu et al, MRM,62,2009,66-76, [3] Cho et al, Med Physics, 15,1988, 7-11, [4] Olsen et al, Radiographics, 20,2000,699-712

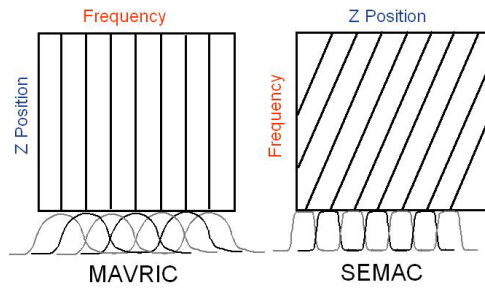


Figure 1: MAVRIC and SEMAC spectral/spatial properties. MAVRIC applies overlapping Gaussian RF without the use of a selection gradient. SEMAC applies a z-selection gradient (tilted frequency/position plane) with adjacent boxcar spectral profiles

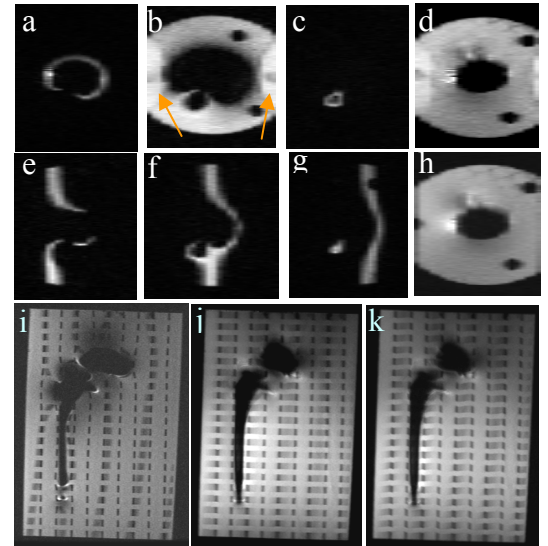


Figure 2: Total hip replacement phantom at 1.5T: a-d) -4 kHz, 0kHz, 4 kHz, and composite reformatted (ky-kz encoded planes) images without use of the z-selective gradient. Arrows indicate aliasing in the kz-encoded dimension. e-h) -4 kHz, 0kHz, 4 kHz, and composite reformatted images using the z-selective gradient. i-k) High-bandwidth 2D-FSE (+/-125 kHz), non-selective, and selective in-plane MAVRIC images.

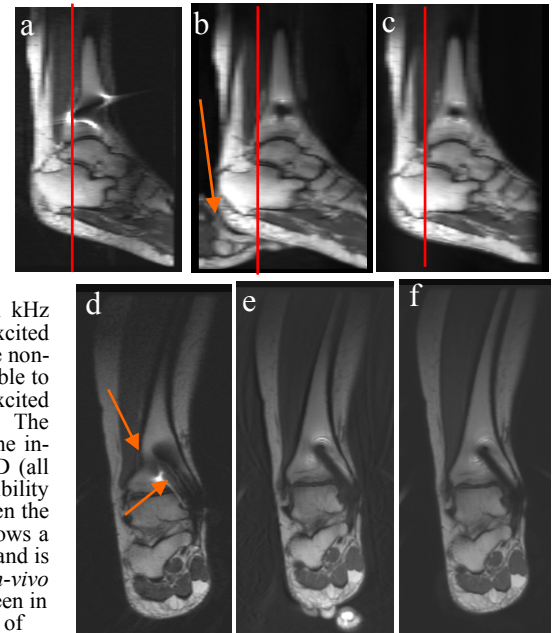


Figure 3: Stainless steel ankle screw at 3T: a) Reformatted 2D-FSE image. b) nonselective and (c) z-selective reformatted (kx-kz encoded planes) MAVRIC images. Arrows indicate aliasing in the kz-encoded dimension in the non-selective image. d-f) In-plane coronal images indicated by red lines in (a-c). Arrows indicate significant distortions in the high-bandwidth 2D-FSE (d) image that are corrected in both the non-selective (e) and z-selective (f) MAVRIC images.